Collection of Correlated Information from Superimposed Multiple Chirp Signals

Koki Aoyama* and Koichi Adachi*
* Advanced Wireless and Communication Research Center, The University of Electro-Communications, Tokyo, Japan
E-mail: {aoyama, adachi}@awcc.uec.ac.jp

***Abstract*—Wireless Sensor Networks (WSNs) based on Long-Range Wide Area Networks (LoRaWAN) are being used in various applications. In WSNs, in addition to periodic packet transmission, sensor nodes transmit packets when they detect an event. This action enables real-time information aggregation. When multiple sensor nodes detect an event at the same time, they send signals simultaneously, which may result in signal collisions at the receiver. This paper proposes a symbol detection method that allows information aggregation even when the GW receives superimposed chirp signals. Furthermore, this paper introduces an event source estimation method as a use case for collecting aggregate correlated information. Computer simulation results show that the proposed method increases the probability of achieving the absolute source estimation error of 10 degrees by 11 points compared to conventional methods.**

I. INTRODUCTION

Advances in wireless communication technology have led to the use of the Internet-of-Things (IoT) in a variety of fields. In particular, the IoT-based Wireless Sensor Networks (WSNs) technology has attracted attention, and various research works have been conducted in both industrial and academic fields [1]. WSN is a network consisting of many sensor nodes with wireless communication capability and a GateWay (GW) that collects information from the sensor nodes. Sensor nodes consisting of WSN are preferred to be inexpensive because they are installed in many locations. Due to environmental constraints, they are usually powered by batteries. Therefore, maintenance costs and battery life are important in WSN, and communication systems with low power consumption are preferred [2]. One of the communication systems used in WSN is the Long-Range Wide Area Network (LoRaWAN). LoRaWAN enables long-range communication with low power consumption by adopting Chirp Spread Spectrum (CSS) modulation as its physical layer technology. Furthermore, since LoRaWAN operates in the unlicensed band, it is used in various WSN scenarios [3], [4].

Local regulators introduce several restrictions, including maximum Time-on-Air (ToA) per transmission and Duty Cycle (DC) to prevent uncontrolled use of the frequency bands. DC limits the total transmission time during a specific period. In addition, the battery-powered nature of the nodes makes it difficult for them to exchange information with the GW frequently. Thus, information collection in WSNs is often initiated by sensor nodes. The sensor nodes generally periodically transmit the generated packet containing the measured data to the GW. However, periodic transmission cannot handle real-time information collection, such as sudden environmental changes. Therefore, an *event-driven transmission* is introduced in addition to the periodic transmission. In event-driven transmission, sensor nodes transmit the measured data immediately once it satisfies the predetermined criteria. This event-driven transmission allows GWs to detect events and collect real-time information. However, when an event are observed by multiple sensor nodes, they send information to the GW at the same time, resulting in signal collisions. Since nodes in WSN generally do not retransmit signals to save battery, information about events cannot be collected if such signal collision happens.

One approach to this problem is to adjust the transmission timing of each sensor node to avoid signal collision through some techniques, including Carrier Sense (CS). However, CS and corresponding backoff may incur delays for sending nodes to transmit information to the GW, which takes long time to collect information from all nodes. Therefore, this approach is not suitable for LoRaWAN, which requires a long transmission time for each packet transmission. There is an early work that considers simultaneous transmission of multiple nodes such as over-the-air computing-based wireless information aggregation [5] and sequential interference cancellation [6]. These methods enable information collection from multiple nodes through simultaneous transmission. However, the former requires strict time synchronization, while the latter does not consider reception in situations where many nodes transmit the same data simultaneously. Since event-driven packets contain information about the same event detected by sensor nodes, the transmitted data is expected to be the same or at least highly correlated. Therefore, this paper proposes a symbol detection method for superimposed chirp signal waveforms that takes advantage of the characteristics of event-driven data. Through the computer simulation, the proposed method is shown to enable statistical acquisition of event information in a single transmission time. This paper also introduces event source estimation as one of the use cases for exploiting information aggregation through simultaneous transmission.

This paper is organized as follows. Section 2 presents the system model considered in this study. Section 3 describes the considered modulation method, LoRa and chirp signal superposition. Section 4 describes the proposed method. Section 5 shows the results of computer simulations, and Section 6 concludes the paper.

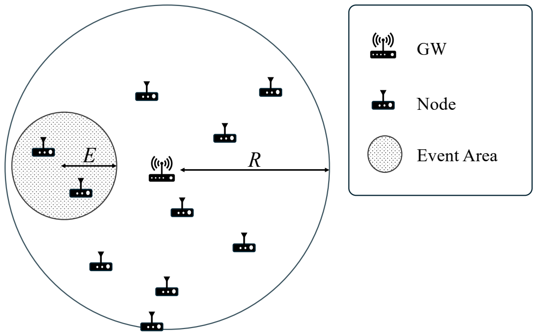

Fig. 1. System model

II. LoRa Modulation & Demodulation

LoRa modulation is based on CSS modulation, which enables long-distance communication with high noise immunity. LoRa signals are characterized by bandwidth W [Hz] and Spreading Factor (SF) S that indicates the number of bits transmitted by one CSS symbol. A high SF improves noise immunity and hence achieves longer communication distance at the cost of longer symbol length. In the following sections, we focus on the physical layer of LoRa and discuss the transmission and reception of chirp signals.

The base up-chirp signal, $\psi_0(t)$, at time t is given by

$$\psi_0(t) = \begin{cases} \frac{1}{\sqrt{2^S}} \left(j2\pi t^2 \frac{W^2}{2^{S+1}} \right) & 0 \le t < T_{\rm s} \\ 0 & \text{otherwise} \end{cases}, \tag{1}$$

where $T_{\rm s} = 2^S/W$ [sec] is the symbol length. Different symbols are represented by cyclically shifting this base up-chirp signal in the time domain. Therefore, the transmitted signal $\psi_m(t)$ of symbol m at time t is expressed as

$$\psi_m(t) = \frac{1}{\sqrt{2^S}} \left(j2\pi \left((t + m \cdot T_{\rm c})_{\bmod T_{\rm s}} \right)^2 \frac{W^2}{2^{S+1}} \right), \tag{2}$$

where $T_{\rm c} = 1/W$ [sec] is the chip length and mod denotes the modulo operation. In the following, we consider the case $0 \le t < T_{\rm s}$ only for notation simplicity.

Once a receiver receives a chirp signal, it performs *dechirping*, *Discrete Fourier Transform (DFT) operation*, and *symbol detection*, which are to be explained in Section III.B in detail.

III. System Model

Figure 1 shows the system model considered in this paper, where N nodes are randomly and uniformly placed within the area of interest with a radius of R [m] centered on the GW. An event occurs at a random location in the area. The nodes, which are located within a radius of E [m] centered on the event location, simultaneously detect the event. Upon detecting the event, a node generates a packet, performs CS, and transmits the generated packet to the GW if it does not detect the ongoing transmission. For simplicity, this paper assumes that nodes transmit event-driven packets only and DC constraints due to periodic transmission are not considered.

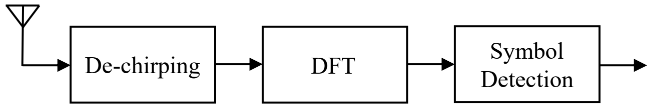

Fig. 2. Receiver model

A. Transmitter Model

Upon detecting the event, a sensor node immediately tries to send the measured data to the GW. The measured value is first quantized into a dicrete value using a predetermined quantization technique. The obtained quantized value is converted to a binary number, which is then modulated to a CSS symbol. This paper does not consider any whitening, channel coding, and interleaving [7]. Therefore, if there is a slight difference or error in the measured value, the neighboring CSS symbols are selected at each transmitter, resulting in multiple neighboring peaks of the DFT output at the receiver.

B. Receiver Model

The simplified receiver model considered in this paper is shown in Fig. 2, which consists of three steps: *de-chirping*, *DFT*, and *symbol detection*.

The chirp signal waveforms transmitted from multiple sensor nodes are superimposed upon the reception at the receiver. Assume that the symbol m is transmitted by multiple nodes (set $\mathcal{A}$) that detected the event. The superimposed signal $r[\ell]$ at the ℓth sampling point can be expressed as

$$r_m[\ell] = \sum_{i \in \mathcal{A}} \sqrt{\frac{P_{{\rm r},i}(d_{{\rm GW},i})}{2}} \psi_m[\ell - \tau_i] + w[\ell], \tag{3}$$

where $P_{{\rm r},i}(d_{{\rm GW},i})$ is the received power of node $i \in \mathcal{A}$ located at $d_{{\rm GW},i}$ [m] away from the GW, $\psi_m(\cdot)$ is the transmitted chirp signal, and $w[\ell]$ is the additive white Gaussian noise (AWGN) that follows $\mathcal{CN}(0, N_0)$ (N_0 is the one-sided power spectral density of the noise).

The τ_i in Eq. (3) denotes the propagation delay for node i. Assume that the internal processing time of all transmitters is constant (or zero). Given event propagation speed $v_{\rm event}$, distance between event source and node $d_{{\rm event},i}$, and distance between node and GW $d_{{\rm GW},i}$, τ_i is determined as follows

$$\tau_i = \frac{d_{{\rm GW},i}}{c} + \frac{d_{{\rm event},i}}{v_{\rm event}}, \tag{4}$$

where c [m/sec] is the speed of light.

The received superimposed chirp signal is subjected to de-chirping, DFT processing, and symbol detection.

a) De-chirping: The de-chirping is carried out as

$$r_m[\ell]\psi_0[\ell]^* = \left\{ \sum_{i \in \mathcal{A}} \sqrt{\frac{P_{{\rm r},i}(d_{{\rm GW},i})}{2}} \psi_m[\ell - \tau_i] + w[\ell] \right\} \psi_0[\ell]^*, \tag{5}$$

where $\{.\}^*$ denotes the complex conjugate operation.

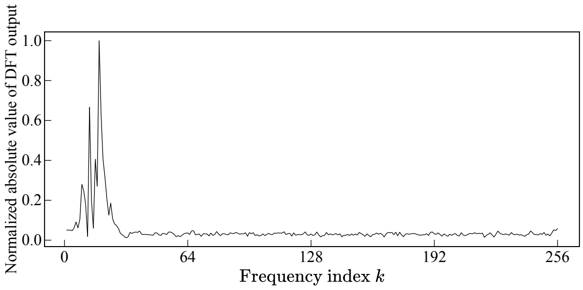

Fig. 3. DFT output spectrum of superimposed received chirp signals.

b) DFT: The kth frequency spectrum obtained by DFT is given by

$$F[k] = \sum_{\ell=0}^{2^S-1} r_m[\ell]\psi_0[\ell]^* \left(-j2\pi\frac{k}{2^S}\ell\right). \tag{6}$$

c) Symbol Detection: The symbol detection at an ordinary LoRa receiver is performed as

$$m^\star = \underset{k\in[0,2,\cdots,2^S-1]}{\text{argmax}} |F[k]|. \tag{7}$$

Conventional symbol detection is optimized for the case where a signal transmitted by a single node is received. When multiple nodes transmit signals simultaneously, the difference in symbols transmitted by each node, propagation delays, and bias in node placement may result in incorrect symbol decision.

IV. Proposed Method

If multiple nodes transmit at the same time, it is likely that they detected the same event. Therefore, the information transmitted by each node is expected to be either the same or at least highly correlated. As described in the previous section, even if there is a measurement error or delay, multiple symbols arrive at the GW within a relatively short time interval. Therefore, if signals from multiple nodes are received simultaneously, the central limit theorem can be used to statistically collect information on events in a single communication time.

This paper proposes a symbol detection method suitable for superimposed chirp signals and an efficient information collection method. Specifically, it aims to improve the symbol detection process after the DFT process to achieve statistically correct symbol detection even when multiple chirp signals are superimposed. We also present an event source estimation as a use case of the proposed symbol detection method.

A. Symbol Estimation

It is highly likely that the DFT output, which usually exhibits a single strong peak, may have multiple peaks within some frequency range due to delay or measurement error. Therefore, the spectrum with the width of the DFT output is used to estimate the transmitted symbols of the superimposed chirp signal. Symbol estimation is difficult because the DFT output is affected by noise in addition to the effect of the superimposed chirp signal. Thus, the proposed symbol estimation method consists of three steps: *noise suppression*, *smoothing*, and *peak width-based symbol detection*.

a) Noise Suppression Step: The noise suppression process is expressed as

$$\alpha[k] = \begin{cases} |F[k]| & \text{if } F[k] > \text{mean}(F) \\ 0 & \text{otherwise} \end{cases}. \tag{8}$$

Since the noise is spread over the entire frequency bandwidth after the dechirping process, the spectrum with a small amplitude value represents highly likely the noise. Thus, this paper uses the average value of DFT output as the threshold to cut out the noise.

b) Smoothing Step: The smoothing is expressed by

$$\begin{aligned}\mu_n[k] = \frac{1}{n}\{\alpha[k] \\ + \sum_{j=1}^{(n-1)/2} \left(\alpha[(k+j)_{\text{mod } 2^S}] + \alpha[(k-j)_{\text{mod } 2^S}]\right)\}.\end{aligned} \tag{9}$$

For a superimposed chirp signal, the DFT output exhibits several consecutive peaks. However, if a small number of sensor nodes transmit simultaneously, the DFT output may have nonconsecutive peaks. Therefore, a smoothing process with a tap number of T is applied to supplement the peak continuity. As the number of smoothing taps, T, increases, the spectrum becomes smoother. However, when the received Signal-to-Noise Ratio (SNR) is low, spectra other than the received signal may appear in the DFT output because the noise suppression process cannot completely suppress the noise. In such cases, if the number of smoothing taps, T, is large, the peaks of the desired signal and those due to noise are indistinguishable, and the estimation accuracy degrades. Thus, the number of taps, T, in the smoothing process may have a significant impact on symbol detection performance.

c) Symbol Detection Step: The post-smoothed spectrum of the superimposed chirp signal is shown in Fig. 4. The figure shows that, in addition to the desired symbol spectrum, some other spectra have relatively large amplitude values due to noise. Therefore, it is necessary to distinguish between the desired signal's spectrum and the noise spectrum. To overcome this difficulty, this paper proposes *peak width-based detection*. The peak width-based detection algorithm is shown in Algorithm 1. Since a LoRa signal is cyclic because it is represented by cyclic shifting the base up-chirp signal, the first half of the DFT spectrum is copied and added to the second half, and then the symbol is determined.

When multiple chirp signals are simultaneously transmitted from multiple sensor nodes, there are time shifts between the received signals due to propagation delay. Thus, the DFT output peak has a width rather than a sharp peak at the desired symbol index, which indicates that the spectra with the largest peak width contain the desired signal's spectrum. Thus, in the proposed peak width-based detection, the DFT spectrum with the largest width is detected as the target spectrum. When only

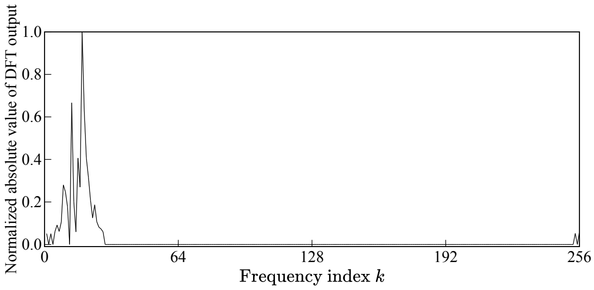

(a) before smooth process

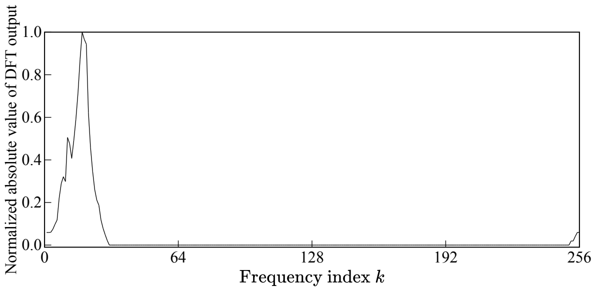

(b) after smooth process

Fig. 4. Smooth process

a single signal is received or when the propagation delay is extremely small, the DFT output peak appears as a single peak. To ensure correct operation even in such cases, when the peak widths of the spectra are the same, the strongest peak is considered as the target spectrum. After deciding the target peak width, the symbol at the center of the peaks is output as the estimated symbol based on the assumption that the superimposed chirp signal obeys the central limit theorem.

B. Event Source Estimation

The proposed method enables symbol detection even for superimposed signals if the correlated information is transmitted. Thus, the receiver cannot detect the data if there is no correlation among the transmitted data such as device IDs. Therefore, this paper considers a way to let the transmitted data have some correlation. In this paper, one method of correlating data is to use the fact that the nodes that detect an event source are located in a circle around the source of the event. Specifically, the device ID is assigned based on the azimuth angle viewed from the GW as

$$\mathrm{dev.ID_H} = \left\lceil \frac{\theta}{2\pi} 2^S \right\rceil . \tag{10}$$

Since there are 3 bytes address prefixes for the device by default as shown in Section V-B, the first 1 byte of the address prefix is assigned to each azimuth angle and the last 2 bytes are used to represent a unique address.

Algorithm 1 Symbol detection :Peak width detection

function PEAKWIDTHDETEC($\mu = [\mu_0, \mu_1, \cdots, \mu_{2^S-1}]$)
  $\mathcal{S} \leftarrow \mathrm{vcat}(\mu, \mu[1 : 2^{S-1}/2])$
  $flag \leftarrow 0$
  for all $index \leftarrow \mathcal{S}$ **do**
    if $\mathcal{S}[index]! = 0$ **then**
      if $flag == 0$ **then**
        $flag \leftarrow 1$
        $tempStart \leftarrow index$
      end if
    else
      if $flag == 1$ **then**
        $flag \leftarrow 0$
        $tempWidth \leftarrow index - tempStart$
        if $tempWidth > indexWidth$ **then**
          $startIndex \leftarrow tempStart$
          $indexWidth \leftarrow tempWidth$
        else if $tempWidth == indexWidth$ **then**
          if $\max(\mathcal{S}[tempStart : index]) > \max(\mathcal{S}[startIndex : startIndex + indexWidth])$ **then**
            $startIndex \leftarrow tempStart$
            $indexWidth \leftarrow tempWidth$
          end if
        end if
      end if
    end if
  end for
  $Symbol \leftarrow startIndex + \mathrm{ceil}(indexWidth/2)$
  return $Symbol \mod 2^S$
end function

V. SIMULATION AND RESULTS

A. Propagation Model

This paper adopts a static channel model that considers path loss and shadowing. The received power, $P_{\mathrm{r},i}(d_{\mathrm{GW},i})$, of node i at GW is calculated as

$$P_{\mathrm{r},i}(d_{\mathrm{GW},i}) = P_{\mathrm{t}} - L_{\mathrm{path}}(d_{\mathrm{GW},i}) - L_{\mathrm{s}}, \tag{11}$$

where P_{t} [dBm] is the common transmit power for all nodes, $L_{\mathrm{path}}(d_{\mathrm{r},i})$ [dB] is space attenuation due to path loss, L_s [dB] is variation due to shadowing. Shadowing is a model that follows a log-normal distribution with spatial correlations [8].

Path loss $L_{\mathrm{path}}(d_{\mathrm{GW},i})$ is calculated using the ITU-R model given by [9]

$$L_{\mathrm{path}}\left(d_{\mathrm{GW},i}\right) = 10\alpha \log_{10}\left(d_{\mathrm{GW},i}\right) + \beta + 10\gamma \log_{10}\left(f_{\mathrm{c}}\right), \tag{12}$$

where α, β, γ are parameters related to path loss and f_{c} is the center frequency of the CSS modulation signals.

B. Frame Format

The LoRaWAN frame format is shown in Fig. 5. The communication standard for LoRaWAN is defined by the LoRa

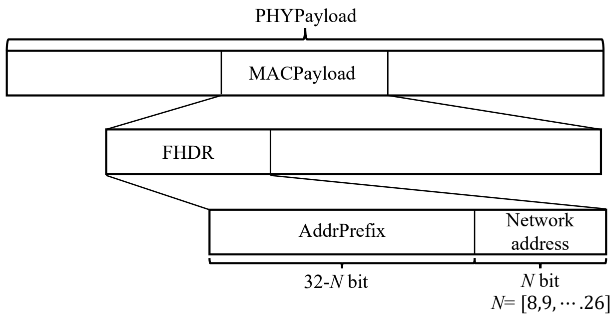

Fig. 5. Frame Format

TABLE I
SIMULATION PARAMETERS

Parameters	Value
Center Frequency f_c	920 [MHz]
Band Width W	125 [kHz]
Spreading Factor S	8
Transmit Power P_t	13 [dBm]
Noise power spectrum density N_0	-174 [dBm/Hz]
Shadowing standard deviation σ^2	7.6
Transmit symbol	10 [Symbol]
Number of GW	1
Number of ENs	1,000
Simulation area radius R	800 [m]
Event area radius E	200 [m]
Number of trials	10^6

Alliance, and the frame format shall also conform to the standard [10]. The device address (4 bytes) is stored in the MAC payload in the frame header.

As shown in Fig. 5, the device address consists of a node unique AddrPrefix and a network address totaling 32 bits and is unique within the network. The length of the AddrPrefix is determined by the length of the network address, which is set to 8 bits (1 byte) [10].

C. Simulation Parameters and Performance Metrics

This section provides computer simulation results to show the effectiveness of the proposed method. The simulation parameters are shown in Table 1. The path loss parameters are set to $\alpha = 4.0$, $\beta = 9.5$, and $\gamma = 4.5$, respectively, assuming communication in a Non-Line-of-Sight (NLoS) environment [9]. Symbol synchronization during reception is assumed to be ideal for the first received signal. In this paper, we adopt the Cumulative Distribution Function (CDF) to characterize the change in information aggregation accuracy with the number of concurrent aggregation nodes and the absolute estimation error of the event source estimation. For the change in information aggregation accuracy with the number of concurrently collected nodes, we assume the mean $\mu = 100$ and variance $\sigma^2 = 5$ due to measurement error, and verify the information collection accuracy when the number of concurrently collected nodes is set to $N = \{1, 10, 100, 1000\}$. For the event source estimation, we evaluate the estimation results and the CDF of the estimation error after 10^6 trials. As a benchmark method, the DFT peak detection given by Eq. (7) is used as the symbol detection method.

D. Simulation Results

Figure 6 shows the impact of the number of transmitting nodes on the absolute error of the event source estimation. The figure shows that information collection accuracy increases with the number of superimposed LoRa signals.

Figures 7(a) and 7(b) show the event source estimation results of the benchmark method and those of the proposed method. Figure 7(b) shows that the proposed method estimate the center of the event source better than the conventional method. Because the proposed method is not affected by the DFT output peak bias due to the superimposed chirp signal.

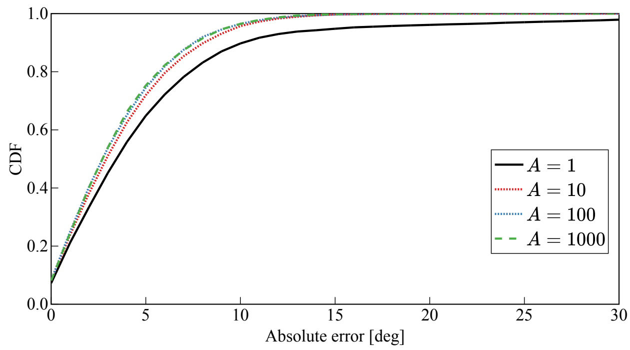

Fig. 6. Impact of the number of superimposed chirp signals on estimation accuracy ($A = |\mathcal{A}|$).

The CDF of the absolute estimation error of the proposed method with varying the number of smoothing taps, T, is shown in Fig. 8. Figure 8 shows that the proposed method outperforms the benchmark method in estimation accuracy; specifically, the proposed method with $T = 5$ taps improves the CDF value by 11 points at ± 10 degrees and by 5 points at ± 15 degrees compared to the benchmark method. The reason why the estimation accuracy differs depending on the number of taps T lies in the fact that the peak width is detected to be wide due to noise or that the smoothing of peaks is insufficient, and the number of taps T in the smoothing process needs to be adjusted according to the average received SNR. In addition, both the benchmark and the proposed methods show an absolute error of ± 30 degrees or more, and there are cases where the event source estimation does not work correctly. This may be due to the fact that the sensor nodes detecting the event are located in the vicinity of the GW and the superimposed signals are composed of uncorrelated data. In the case where the event happened on edge to distributions of end node, estimation accuracy degrades due to SNR degradation, but estimation itself can be performed.

VI. CONCLUSION

This paper examined statistical information collection from superimposed chirp signals transmitted by the nodes that have detected the event. Since the delay of the superimposed signal

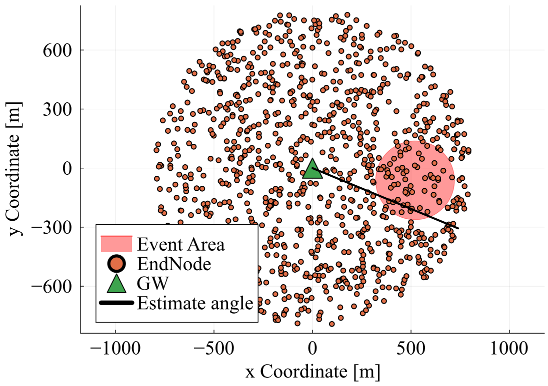

(a) Benchmark method

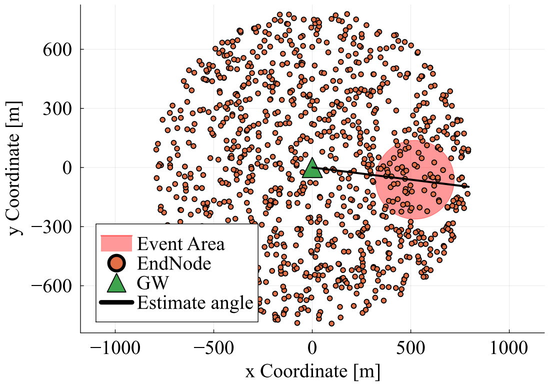

(b) Proposed method

Fig. 7. An example of event source estimation result.

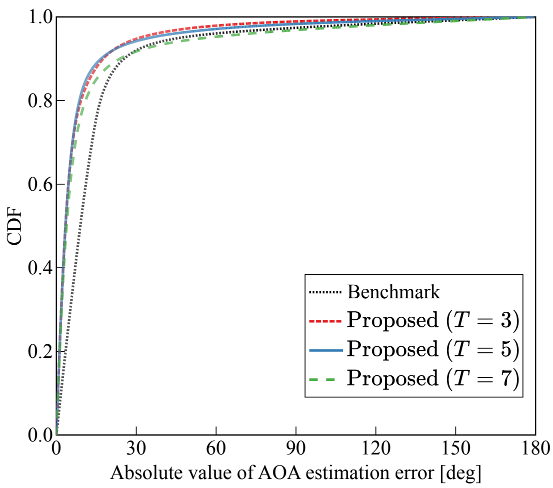

Fig. 8. Impact of smoothing tap T on the absolute estimate error.

degrades the accuracy of information collection, this paper proposed a symbol detection method using the peak width of the DFT spectrum, and event source estimation was identified as a use case. Computer simulation results have shown that the proposed method improves the absolute error in event source estimation by up to 11 points for a CDF value of 10 degrees compared to the conventional symbol detection method, thus improving the accuracy of information collection.

References

[1] K. Thirunavukkarasu, L. Raju, and S. Sathishbabu, "A Survey on LoRaWAN for Smart Medical and Industries," in *2023 9th Int. Conf. on Electrical Energy Systems (ICEES)*, 2023, pp. 34–40. DOI: 10.1109/ICEES57979.2023.10110099.

[2] C. Milarokostas, D. Tsolkas, N. Passas, and L. Merakos, "A Comprehensive Study on LPWANs With a Focus on the Potential of LoRa/LoRaWAN Systems," *IEEE Commun. Surv. Tutor.*, vol. 25, no. 1, pp. 825–867, 2023. DOI: 10.1109/COMST.2022.3229846.

[3] U. Raza, P. Kulkarni, and M. Sooriyabandara, "Low Power Wide Area Networks: An Overview," *IEEE Commun. Surv. Tutor.*, vol. 19, no. 2, pp. 855–873, 2017. DOI: 10.1109/COMST.2017.2652320.

[4] W. Ayoub, A. E. Samhat, F. Nouvel, M. Mroue, and J.-C. Prévotet, "Internet of Mobile Things: Overview of LoRaWAN, DASH7, and NB-IoT in LPWANs Standards and Supported Mobility," *IEEE Commun. Surv. Tutor.*, vol. 21, no. 2, pp. 1561–1581, 2019. DOI: 10.1109/COMST.2018.2877382.

[5] G. Zhu, Y. Du, D. Gündüz, and K. Huang, "One-Bit Over-the-Air Aggregation for Communication-Efficient Federated Edge Learning: Design and Convergence Analysis," *IEEE Trans. Wireless Commun.*, vol. 20, no. 3, pp. 2120–2135, 2021. DOI: 10.1109/TWC.2020.3039309.

[6] J. Bukhari and Z. Zhang, "Simple Peak Interference Cancellation (SPIC): Interference Cancellation Prior to Packet Decoding in LoRa Networks," in *2023 IEEE Latin-American Conf. on Commun. (LATINCOM)*, 2023, pp. 1–6. DOI: 10.1109/LATINCOM59467.2023.10361900.

[7] M. Jouhari, N. Saeed, M.-S. Alouini, and E. M. Amhoud, "A Survey on Scalable LoRaWAN for Massive IoT: Recent Advances, Potentials, and Challenges," *IEEE Commun. Surv. Tutor.*, vol. 25, no. 3, pp. 1841–1876, 2023. DOI: 10.1109/COMST.2023.3274934.

[8] Z. Wang, E. K. Tameh, and A. R. Nix, "Joint Shadowing Process in Urban Peer-to-Peer Radio Channels," *IEEE Trans. Veh. Technol.*, vol. 57, no. 1, pp. 52–64, 2008. DOI: 10.1109/TVT.2007.904513.

[9] ITU-R Recommendation P.1411-12, "Propagation data and prediction methods for the planning of short-range outdoor radiocommunication systems and radio local area networks in the frequency range 300 MHz to 100 GHz," Sep. 2021.

[10] LoRa Alliance, "LoRaWAN Certification Protocol Specification TS009-1.0.0," 2020.